Zárójelentés

"Poli(N-izopropilakrilamid) alapú mikrogélek elektromos tulajdonságai és kölcsönhatása ionos tenzidekkel"

(OTKA K 100762)

A kutatás célja, a kutatási program ismertetése

A mikrogélek (nanogélek) rendkívül széleskörű alkalmazási lehetőségük miatt az utóbbi évtizedekben a kutatásokban kiemelt figyelmet kaptak. Elsősorban az un. „intelligens" anyagok kerültek az érdeklődés központjába duzzadási tulajdonságaik és permeabilitásuk külső paraméterek (mely a gél kémiai összetételétől függően lehet a hőmérséklet, ionerősség, pH, elektromos tér, stb.) hatására történő extrém nagymértékű és reverzibilis változása miatt. Bár számos intelligens anyag készítésére alkalmas polimert találtak, ezek között is különösen fontossá váltak a hőmérséklet-érzékeny poli(N-izopropilakrilamid) (pNIPAM) mikrogélek (Pelton, R. H. *Adv. Colloid Interface Sci*. **2000**, *85*, 1.), melyek 34 ^{o}C körül egy szük hőmérséklet-tartományban kollapszust szenvednek. A csak akrilamid monomerből, vagy más egyféle monomerből felépülő mikrogélek felhasználhatóságát azonban korlátozza a kémiai minőség által meghatározott kollapszus hőmérséklet. A mikrogél tulajdonságainak változtatására további lehetőségek: kopolimer gélek szintetizálása, mag-héj szerkezetű mikrogélek előállítása és a polimerrel erősen kölcsönható adalékokkal a rendszer tulajdonságainak módosítása.

A kopolimerizációval történő módosítás különösen akkor jelentős, ha a ko-monomer minősége lényegesen eltérő, pl. a NIPAM-ot akrilsav monomerrel együtt polimerizáljuk. Ebben az esetben a hőmérsékletérzékeny pNIPAM a beépült gyenge savként viselkedő akrilsav jelenlétében további paraméterek, a pH és az ionerősség változására is reagál, és a kollapszus hőmérséklet is eltolódik.

A mag-héj felépítésű szerkezetek a mikrogélek sziporkázóan sokféle felhasználására nyitnak újabb lehetőséget. Az első szintézisben készített magra egy következő lépésben az eltérő összetételű héjat polimerizálják rá. Ebben a csoportban szintén azoknak az anyagoknak van nagyobb jelentősége, melyekben a mag és héj polaritása eltérő. Pl. az egyik NIPAM monomerekből, a másik akrilsavból épül fel. Meg kell itt emelíteni, hogy kb. 25 %-nál több akrilsav monomert nem lehet sem a magba sem a héjba beépíteni, mert afelett a mikrogél szintézise anomálissá válik.

Az adalékokkal történő módosítás szempontjából elsősorban a tenzidek jönnek szóba. Az akrilsavas izopropilakrilamid kopolimerek vagy a mag-héj szerkezetű

gélek az ellentétes töltésű ionos tenzidekkel erős kölcsönhatásba lépnek és alapvetően módosítják azok elektromos tulajdonságait.

A mikrogélek elektromos tulajdonságainak jellemzésére jelenleg egyetlen módszer, a részecskék elektroforetikus mozgékonyságának mérése áll rendelkezésre. Az elektroforézis értékelésére kétféle, egymásnak koncepcionálisan ellentmodó elmélet használatos, ezek a klasszikus kompakt kolloid részecske („non-draining") modell és a szabad átfolyásos („free draining") modell. A mikrogél részecskék elektoforetikus mozgékonyságának elméleti leírásával kapcsolatban a nehézség abban rejlik, hogy az ellenőrzéshez szükséges független elektromos paraméter jelenleg nem mérhető, ráadásul az elektromosan „semleges" pNIPAM is tartalmaz a szintézis során alkalmazott perszulfát iniciátorból származó szulfát csoportokat. Az irodalomban megjelent közlemények túlnyomó többségében a priori az un. „free draining" modell alapján értelmezik a mozgékonyságot és az elmélettől való eltéréseket megalapozatlan korrekciókkal próbálják magyarázni. Ebben az elméletben, mivel a mozgékonyság a részecske összes töltésével kapcsolatos, a klasszikus elméletből számolható felületi potenciálnak nincs is fizikai tartalma. A mikrogél-tenzid és polielektrolit-tenzid részecskék mozgékonyságának értékelése során az ezen rendszerekkel foglalkozó közlemények a free draining modellről tudomást sem vesznek, hanem a klasszikus elmélet alapján kvalitatív szinten interpretálják a méréseket. A klasszikus modell sem lenne azonban alkalmazható eredeti formájában, mert a mikrogél részecskék nem kompaktak és a kisionok behatolhatnak a részecskék felületi töltés-rétegébe.

Kutatásaink elsődleges célja a részecskék elektromos jellemzése volt jól definiált modelleken végzett szisztematikus mérések alapján, annak eldöntésére, hogy melyik koncepció a korrekt, azaz mi a döntő paraméter (a részecske összes töltése vagy a felületi töltés), amely a mozgékonyságot meghatározza. Különböző elektromosan töltött és semleges mag-héj szerkezetű gélrészecskéken történő vizsgálatokkal kívántuk kvalitativ szinten eldönteni, hogy az elektroforetikus mozgékonyság értelmezésére melyik koncepció használható, azonban ezek sem bizonyultak a kérdést egyértelműen eldöntőnek. A különböző szerkezetű részecskék mozgékonysága ugyanis csak akkor volt értelmezhető ugyanazon elmélet keretein belül, ha feltételeztük, hogy a töltött mag/semleges héj esetében a mag duzzadása során a mag ionos polimerláncai részlegesen penetrálnak a semleges héjba. Ennek eldöntése céljából ugyanarra a p(NIPAm-co-akilsav) töltött kopolimer magra különböző vastagságú semleges pNIPAM héjat épitettünk. Vizsgáltuk továbbá a különböző polielektrolit-ellentétesen töltött ionos tenzid rendszerek oldatbeli és határfelületi tulajdonságait.

A kutatás során elért eredmények

1. Mikrogél modellek előállítása és az ahhoz kapcsolódó eredmények

Különböző pNIPAM mikrogél latexeket szintetizáltunk, a mintákat tisztítottuk (dialízis, centrifugálás) és hidrodinamikai méret, valamint kollapszus hőmérséklet mérésekkel jellemeztük.

a/ Előállítottunk egy adott keresztkötés-sűrűségnél heterogén szegmenseloszlású pNIPAM mintát a hagyományos "bath" módszerrel, valamint homogén szegmenseloszlású mintát az általunk korábban kidolgozott új "feeding" módszerrel (Roberta Acciaro, Tibor Gilányi and Imre Varga, Langmuir 2011, 27, 7917–7925). Megállapítottuk, hogy a részecskék szegmens-eloszlása a kollapszus hőmérsékletre nem hat számottevően, a duzzadási tulajdonságok azonban nagymértékben változnak.

b/ Mag/héj szerkezetű (töltött NIPA-co-akrilsav kopolimer mag semleges NIPA héjjal és semleges mag töltött héjjal) mintákat állitottunk elő. A hagyományos mag-héj szintéziseket két lépésben végzik: előbb a magot állítják elő, szeparálják, tisztítják, majd azokon polimerizálják a héjat. A héj fizikailag kapcsolódik a héjhoz. Ezzel a módszerrel legfeljebb 25% akrilsavtartalmú kopolimer héjat lehet felépíteni. A mag-héj szerkezet előállítására új, egylépéses szintézis módszert dolgoztunk ki, melynek előnye nemcsak egyszerűsége, hanem az is, hogy a héj kémiai kötésekkel kapcsolódik a maghoz, továbbá 100 % akrilsavtartalmú héj is szintetizálható. A polielektrolit héj képezhető keresztkötésekkel vagy anélkül, továbbá hagymaszerkezetű komplex mikrorészecskék (A-B-A-B... vagy A-B-C-D...) is előállíthatók, amely az alkalmazási lehetőségek szélesebb körét nyitja meg.

Meghatároztuk a duzzadásfok vs. hőmérséklet függvényeket, valamint az elektroforetikus mozgékonyságot a kollapszushőmérséklet alatt és felett.

c/ A mikrogél részecskék elektroforetikus viselkedésében mutatkozó ellentmondás tisztázása érdekében pNIPAM homopolimerrel boritott töltött mag/semleges héj szerkezetű mikrogél részecskék növekvő héjvastagságú sorozatát állítottuk elő. A különböző monomereknek a polielektrolit gélbe történő konverzióját HPLC mérésekkel követtük az idő függvényében. A szintézis első szakaszában a polielektrolit magot szintetizáltuk, majd az akrilsav teljes beépülése után csak NIPAM momomert tartalmazó rendszerben folytattuk a szintézist a semleges héj kiépítése céljából. A héj növekedése során mintát vettünk a reakcióelegyből, a polimerizációt leállítottuk és a mikrogél szeparálását és tisztítását követően DLS és elektroforézis méréseket végeztünk.

2. Mikrogélek elektromos tulajdonságainak vizsgálata

Az elektromosan semleges pNIPAM, a 10 % akrilsav tartalmú töltött NIPAM-akrilsav kopolimer, továbbá a semleges pNIPAM magon töltött héj és a töltött magon semleges héj szerkezetű mag-héj mintákon dinamikus fényszóródás és elektroforetikus mozgékonyság méréseket végeztünk a hőmérséklet függvényében állandó ionerősségnél pH = 7-nél, amikor az összes akrilsav disszociált állapotban van. Vizsgáltuk továbbá a pNIPAM magon növekvő vastagságú semleges héjat tartalmazó minták elektroforetikus mozgékonyságát.

A töltött részecskék térfogata egy nagyságrenddel nagyobb mint a semlegeseké. Egyezésben az általános irodalmi tapasztalattal, a részecskék hidrodinamikai mérete csökken a hőmérséklet növekedésével. A semleges pNIPAM részecskék 32 ^{o}C körül kollapszust szenvednek. A töltött részecskék kollapszus hőmérséklete nagyobb hőmérséklet felé tolódik és a kollapszus elnyújtottá válik. Meglepő módon a semleges mag – töltött héj és a töltött mag – semleges héj szerkezetű mag-héj minták részecskeméret vs. hőmérséklet függvénye nem különbözik.

A méréseket a szabad átfolyásos és a kompakt részecske modell alapján értékeltük. A modellek fizikai alapját elméletileg is elemeztük és skálázási érvelés alapján megmutattuk, hogy a részecskék mozgását meghatározó hidrodinamikai ellenállás nagyságrendekkel nagyobb a szabad átfolyásos modell esetén, amikoris az összes polimerszegmens surlódik, szemben azzal, ha a részecske kompakt kinetikai egységként mozog. Ez az eredmény egyezik a polimerreológiából jól ismert koncepcióval, miszerint oldatban a polimergombolyag a benne lévő oldószerrel együtt mozog.

Eltérően a korábbi irodalmi gyakorlattól, nem a mozgékonyságot számoltuk az elméletekből a mérési adatokkal való összehasonlítás céljából, amihez több bizonytalan paraméter szükséges, hanem a töltést. A megvalósított kísérleti körülmények között a részecskék töltése ugyanis a duzzadási foktól függetlenül állandó érték. Ezért függetlenül attól, hogy az elméletileg a kétféle modellből számolt töltés abszolut értéke a számoláshoz használt paraméterek esetén korrekt-e vagy sem, az elméletileg számolt töltésre a részecskék duzzadási fokától független invariáns értéket kell kapni, ha az elmélet korrekt. A kisérleti mobilitásokból számolt töltés a duzzadásfok fügvényében mind a négy vizsgált mikrogél esetében konstans a felületi töltés modellből számolva. A szabad áramlásos modell viszont jelentős növekedést mutat a részecskék méretének növekedésével. Megállapítottuk, hogy a kompakt részecske modell alkalmasabb a mikrogél részecskék elektroforetikus mozgékonyságának értelmezésére.

(A munka eredményéről a Langmuirnak beküldött kézirat a beszámoló végén mellékletben csatolva van.)

3. Polimer-tenzid és polielektrolit-tenzid rendszerek vizsgálata

a/ Vizsgáltuk a poly(diallyldimethylammonium chloride)/sodium dodecyl sulfate (Pdadmac/SDS) and poly(ethylene imine)/SDS (PEI/SDS) elegyeket dinamikus felületi feszültség, ellipszometria, Brewster mikroszkópia és neutron reflektometria mérésekkel. Mivel bizonyos összetétel tartományban a tömbfázisban nemegyensúlyi aggregátumok képződnek, a rendszereket többféle keverési eljárással állítottuk elő és vizsgáltuk a levegő/oldat határfelületi tulajdonságokat.

Az ellentétes töltésű polielektrolit-tenzid komplexek oldatbeli és határfelületi tulajdonságainak vizsgálata során megállapítottuk, hogy bizonyos összetétel tartományban, amikor nem-egyensúlyi rendszerek képződnek az oldatban, a komplex spontán behatol az adszorpciós rétegbe. Ezért az adszorpciós réteg szerkezete nemcsak a rendszer összetételétől, hanem az előállítás módjától és az időtől is függ. Ez magyarázatot ad az ilyen rendszereken végzett mérések és az ezeket tartalmazó ipari termékek rendkívül rossz reprodukálhatóságára és ismerete lehetőséget ad a tulajdonságok megbízható szabályozására.

b/ Polielektrolit-tenzid filmek ultrahatékony előállítása oldatból elektromosan semleges komplexek szétterítésével.

Vizsgáltuk a poly(sodium styrene sulfonate)/dodecyl trimethylammonium bromide (NaPSS/DTAB) polielektrolit/tenzid rendszert elektroforetikus mozgékonyság mérésekkel, valamint ezek elektromosan semleges összetételű komplexét a levegő/oldat határfelületen Langmuir filmmérlegben ellipszometria mérésekkel.

A polielektrolit-tenzid részecskék oldatból a határfelületi rétegbe kerülésének kinetikáját és a képződött filmek tulajdonságait vizsgáltuk. Megállapítottuk, hogy a korábbi nézettel ellentétben a filmek tulajdonságait nem lehet egyensúlyi állapotokkal értelmezni. Vizsgáltuk a filmek dinamikus tulajdonságait és arra alapozva egy új módszert mutattunk be ultrahatékony filmek előállítására, melynek alkalmazásával a rendszer összes makromolekula-tartalmának harmada kerül a felületi filmbe, akkor is, ha a makromolekula tenzid nélkül nem felületaktiv. A film első kompressziójakor a filmből a felesleges anyag eltávozik, majd a további kompressziók során oldhatalan filmként viselkedik. Ezek az eredmények paradigmaváltást jelenthetnek e filmek ipari előállításának kiaknázásában mind a filmek tulajdonságainak beállításában, mind a környezetkárosítás vonatkozásában.

c/ Poli(vinilalkohol-vinilszulfát) kopolimer hexadecil- és dodecil ammónium bromiddal képezett komplexeit vizsgáltuk pirén fluoreszcencia spektroszkópia, elektroforetikus mozgékonyság, turbiditás és dinamikus fényszóródás mérésekkel.

A mérési eredmények arra utalnak, hogy a tenzid polielektrolithoz való kötődése három tartományra bontható. Kis tenzidkoncentrációknál a tenzid a szulfát csoportokhoz kötődik és a rendszer valódi oldat. A töltéssemlegesítődés tartományában kompakt kolloid részecskék keletkeznek, melyek koagulálnak. További tenzidadalék hatására a részecskék. Korábbi kutatásaink alapján, ha a komplex homopolimert tartalmaz, akkor kis ionerősségnél kinetikailag stabil kolloid rendszer képződik és további változás már nincs a rendszer állapotában növekvő tenzidkoncentrációval. A vizsgált kopolimer esetében azonban egy bizonyos kritikus tenidkoncentráció felett a tenzidnek a vinilalkohol csoportokkal való kölcsönhatása következtében a kompakt részecskék újra megduzzadnak és ismét termodinamikailag stabil polimer-tenzid oldat képződik, mint a kölcsönhatás első szakaszában.

4. Mikrobuborékok előállítása

A nanorészecskék elektromos tulajdonságainak vizsgálata céljából mérési terveinket egy új elképzeléssel bővitettük, amely az elektromos tulajdonságok alaptudományi vizsgálatához és esetleg újabb gyakorlati felhasználásokhoz adhat lehetőséget. Az elképzelés lényege, hogy néhány száz nm méretű stabil "nanobuborékokat" (mikrobuborékokat) tartalmazó gázdiszperziót állitunk elő, melyek levegő/oldat határfelületén tenzideket adszorbeáltatunk, majd a továbbiakban komplex mikrobuborék/mikrogél rendszereket állitunk elő és azok tulajdonságait elektroforetikus és dinamikus fényszórás módszerrel vizsgáljuk. A makroszkópos felületen adszorbeált tenzidréteg elektromos tulajdonságairól (pl. az ellenionok szerepéről) megfelelő mérési módszer hiányában ugyanis jelenleg nincs megbizható ismeret.

Ultrahang generátor segitségével mikrobuborékokat állítottunk elő és vizsgáltuk az előállitás optimális paramétereit. A mikrobuborékokon adszorbeált ionos tenzidek elektroforetikus mozgékonyságának vizsgálatára során azt tapasztaltuk, hogy a minták nem-fölöződő, valószínűleg a buborékok előaprításához beépített szerves szűrőből származó részecskékkel szennyezettek. Miután a mérésből az üveg-küvettán kívül minden idegen anyagot kiküszüböltünk, kiderült, hogy a titánfej a koncentrálódó nagy energia miatt szintén apritódik, amit vizuálisan is látható gyors kopása is igazol. Ezt a problémát a gázdiszperzió utógos centrifugálással történő szeparációjával próbáltuk megoldani. A kapott „gázdiszperzió" szedimentációs stabilitása azonban elméletileg sem titánrészecskékkel, sem buborékokkal nem értelmezhető. Valószinüleg titánt is

tartalmazó buborékok keletkeznek a rendszerben. Ennek a témának a jövőbeli folytatásához az ultrahangos módszer helyett más módszert (pl. elektrolízis, hirtelen nyomásváltoztatás) kell a buborékok előállításához választani.

Kutatási eredményeinkről a polielektrolit-tenzid kölcsönhatás témakörben vezető folyóiratokban 2 közlemény megjelent az OTKA támogatás feltüntetésével. Két további közleményt a mag-héj szerkezetű mikrorészecskék elektroforetikus mozgékonyságáról és polielektrolit-ionos tenzid monorétegekről benyújtottunk. A mikrogélek elektromos tulajdonságainak témakörében elvégzett kísérletek anyagából további publikációk az értékelés elméleti alapját megalapozó dolgozat megjelenését követően kerül sor.

A Langmuirnek beküldött dolgozat kézirata

Effect of internal charge distribution on the electrophoretic mobility of poly(*N*-isopropyl acrylamide) based core-shell microgel particles

Imre Varga*, Attila Borsos and Tibor Gilányi

Laboratory of Interfaces and Nanosized Systems, Institute for Chemistry, Eötvös Loránd University, P.O. Box 32, H-1117 Budapest, Hungary

Abstract

The electrophoretic mobility of poly(*N*-isopropyl acrylamide) and poly(*N*-isopropyl acrylamide -co-acrylic acid) copolymer particles, as well as different core-shell microgel particles (neutral core with charged shell and charged core with neutral shell) was investigated. The size of the particles was changed by de-swelling the microgels with increasing the temperature. To interpret the experimental results we used scaling arguments to show that due to the strong hydrodynamic interactions the inner part of the microgel becomes non-draining in low ionic strength media and only the outmost thin shell of the microgel contribute actively to the electrophoretic mobility. We found that the experimental results were in good agreement with prediction of this model, while we found physical inconsistencies when the experiments were analysed in terms of the draining models used wide-spreadly in the literature.

INTRODUCTION

In recent years, considerable interest has been focused on the development of "smart" aqueous microgels whose properties change dramatically upon the application of a specific environmental stimulus (e.g. temperature change). While a variety of polymer systems have been explored, most attention has been payed to microgels that are based on poly(*N*-isopropyl acrylamide), pNIPAm.[1] Despite the fact that the charge distribution within the microgel particles has a profound effect on their properties (e.g. swelling and colloid stability) the possibilities for the characterization of the electrical structure of the microgel particles is rather limited. The total charge of the particles can be measured either by conductometric or potentiometric titration.[2] However, these measurements may only provide limited information on the charge distribution within the particle. Another widely used

method to characterize the electrical properties of the microgel particles is to measure their electrophoretic mobility. These data provide crucial information to understand the colloid stability of these systems. However, if we are interested in the relationship between the mobility and the charge distribution within the soft gel particles the available literature seems rather ambiguous. Two concepts have been used to interpret the experimental mobility data of the microgel particles. Either the gel beads are treated as non-draining hard sphere colloids[3] or as spherically symmetric, draining polyelectrolytes[4] that are permeable to the solvent and mobile charged species. In the former case the electrophoretic mobility is determined by the electrokinetic charge (charges localized at the surface of the particle; i.e., the amount of charges, which are compensated beyond the slipping plane of the moving particle in the diffuse electric layer). However, in the latter case all fixed charges embedded into the gel network contribute to the mobility of the gel beads (for further details see below).

In the very first paper that investigated the temperature dependence of the electrophoretic mobility of pNIPAm microgel particles, Pelton et al.[3] have already used both a polyelectrolyte and a colloid particle model to fit the experimental mobility data. They concluded that though the surface charge model required 20 times less charge in a particle, the two fitted theoretical models resulted in rather similar curves that were in reasonable agreement with the experimental data.

Ohshima et al.[5] studied the electrophoretic mobility of polystyrene particles covered by a pNIPAm shell as a function of the ionic strength. They concluded that the draining model well describes the mobility below and above the LCST temperature of pNIPAm. However, it should be noted that when pNIPAm is in its collapsed state its water content reduces below 50%,[6] thus it is rather questionable if the medium can indeed drain through the collapsed gel particle under these circumstances. Later, an extensive study was performed by Pichot et al.[7] on the electrophoretic mobility of latex particles composed of a polystyrene core and a pNIPAm or poly(NIPAm-co-aminoethyl methacrylate) shell. They measured the mobility of the latex particles as a function of pH, temperature and ionic strength. They concluded that the uniform polyelectrolyte layer model proposed by Ohshima could not describe their experimental data at low ionic strength but it worked at high salinity. They attributed this discrepancy to ionic strength induced charge distribution changes within the latex particles.

Fernandes et al. has investigated the electrophoretic mobility of ionic microgel particles (2-vinylpyridine crosslinked with divinylbenzene) as a function of pH in 1 mM NaCl.[8] They used Ohshima's theory for polyelectrolyte coated spherical particles[4] to model the experimental mobility data. As they highlighted in this paper the main challenge in the application of the draining polyelectrolyte models is that the hydrodynamic friction of the polyelectrolyte network usually cannot be calculated as the sum of the independent Stokes friction of the polyelectrolyte segments. To overcome this difficulty they used an empirical function to describe the friction coefficient with changing polymer volume fraction in the gel particle. Finally they concluded that the model can provide a qualitative description of the experimental data but quantitative fitting would require further refinements. In a next paper they also investigated the electrophoretic mobility of the same microgel particles as a function of the ionic strength both in the swollen and the collapsed state.[9] They arrived to the conclusion that the microgels behave as free-draining spherical polyelectrolytes in their swollen state and as charged hard spheres when they are collapsed.

Hoare et al. went one step further and investigated the electrophoretic mobility of microgel particles having identical overall charge but different internal charge distributions. Namely, they prepared carboxylic group containing microgel particles where the charges resided at or near the microgel surface (methacrylic acid/pNIPAm copolymer microgel) as well as microgels that incorporated more than one third of the carboxylic groups inside the gel beads (hydrolyzed acrylamide/pNIPAm copolymer microgels). They measured the mobility of the microgel particles in 1 mM KCl as a function of pH.[2] The most interestingly they found that in a pH range where carboxylic groups got charged in the core of the gel particles only particle swelling occured but significant mobility change could not be detected. At the same time when the charges are localized at the particle surface both particle swelling and increasing electrophoretic mobility can be observed in the relevant pH range. These results imply that only the surface charges contribute to the electrophoretic mobility of the gel particles. It should also be mentioned that similar results were found when the binding of an ionic surfactant (sodium dodecyl sulfate) was investigated to pNIPAm microgels. In that case the electrophoretic mobility of the gel beads also showed changes only when the surfactant binding was going on into the loosely crosslinked outer shell of the microgels.[10] Later Hoare at al. extended their investigation to an even wider range of microgel particles by using comonomers that accumulated in the shell of the microgels (vinylacetic acid and acrylic acid). They investigated the electrophoretic mobility of the non-functionalized pNIPAm and all four types of carboxylic acid functionalized microgels as a function of ionic strength and temperature.[11] Remarkably they observed non-zero plateau mobility values as a function of increasing ionic strength even for the non-functionalized pNIPAm in the fully collapsed state of the microgel particles. Based on these results they concluded that the pNIPAm-based microgel particles behave as soft (draining) particles even well above their collapse temperature. Based on this result they used Ohshima's model to acquire morphological information about the gel particles.

As it is shown by the above summary the literature results are rather contradicting in the question if the microgel beads behave as draining or non-draining particles during electrophoretic mobility measurements. The main difficulty in testing these models is that as it has been highlighted by Penfold[1,3] if suitable fitting parameters are chosen than both models can reproduce the experimental mobility values of the microgel particles. The motivation of our work was to gain further insight how the charges incorporated into the microgel particles contribute to the electrophoretic mobility of the gel beads and to test if either of the draining or the surface charge model could provide a physically consistent description of the experimental data. To achieve this goal we prepared a pool of pNIPAm-based microgel particles with different but well-defined charge distributions: 'uncharged' pNIPAm particles, 'uniformly charged' pNIPAm-co-10%AAc particles and core shell particles with either uncharged pNIPAm core and charged pNIPAm-co-10%AAc shell or charged pNIPAm-co-10%AAc core and 'uncharged' pNIPAm shell were prepared. We measured the electrophoretic mobility and hydrodynamic size of these microgel particles as a function of temperature. Finally, instead of fitting the mobility values using the charge density and the electrophoretic softness as free fitting parameters, an invariant quantity, the 'electrokinetic charge' of the microgel particles was calculated from experimental data and the variation of the particle softness was determined as a function of microgel swelling. Furthermore, based on recent literature results[12,13] we present scaling arguments that imply that only the charges present in a thin draining shell of the microgel contribute actively to the electrophoretic mobility while the inner part of the gel beads acts as a neutral hard sphere. We show that the experimental data are in good agreement with this physical picture.

EXPERIMENTAL

Materials

N-isopropylacrylamide (NIPAm), methylene bisacrylamide (BA), ammonium persulfate (APS), and dodecyl benzene sulfonic acid sodium salt (DBSNa) were provided by Sigma-Aldrich. *N*-isopropylacrylamide was recrystallized from hexane, methylene bisacrylamide was recrystallized from methanol and stored under nitrogen atmosphere in a freezer before use. The other chemicals were used as received. All water used in the preparation, purification and characterization of the microgel particles were taken from a Millipore Milli-Q Integral system purified to a resistance of 18 MΩ, and filtered through a 0.2 μm filter to remove particulate matter.

Uniform microgel preparation

The polymerization was based on the free-radical, precipitation polymerization method developed by Wu et al.[14] for the preparation of monodisperse pNIPAm nanogel particles. A total of 2.85 g of NIPAM monomer, 129 mg of BA, and 46 mg of DBSNa were dissolved in 190 ml distilled water. The temperature of the reactor was kept at 80 ^{o}C, and the solution was intensively stirred. To remove oxygen, nitrogen gas was purged through the solution for 30 min. Then 2 ml of a 2.80 wt% aqueous APS solution (56 mg) was added to the solution, followed by intensive stirring for 4 h. The above protocol was also used to prepare p(NIPAM-co-AAc) copolymer latex particles but in this case, 10 mole% of the NIPAm monomer was replaced by acrylic acid (see Table 1). The pNIPAm latex was purified from unreacted monomers and surfactant by extensive dialysis against Milli-Q water for 4 weeks giving supernatant conductivity of less than 5 μS/cm.

Preparation of core-shell microgel particles.

The core-shell copolymer particles were produced by a two-stage method described by Jones et al.[15] The synthesis of the core particles was performed as described above using only half of the monomers in the polymerization. The shell was added to the purified core particles in a second polymerization step. In the shell synthesis the same amount of monomers were used as in the core synthesis to gain final products where the monomer content of the core and the shell is approximately the same. Furthermore, the total amount of polymer segments (core plus shell) was the same as in the uniform particles. It should be noted that both the core and the core-shell microgels were the subject to the same purification procedure as the uniform microgels particles. However to gain a sufficiently concentrated microgel solution to perform the shell synthesis the dialysed core particle solution was concentrated using a VivaFlow200 ultrafiltration device.

Dynamic Light Scattering Measurements.

The dynamic light scattering measurements were performed by means of Brookhaven dynamic light scattering equipment consisting of a BI-200SM goniometer and a BI-9000AT digital correlator. An Omnichrome (model 543) argon-ion laser operating at 488 nm wavelength and emitting vertically polarized light was used as the light source. The signal analyser was used in the real-time "multi-τ" mode. The time axis is logarithmically spaced over a time interval ranging from 1 μs to 0.1 s. The correlator used 218 time channels. The pinhole was 100 μm. The measurements were performed at a 90 degree scattering angle. Prior to the measurements, the nanogel samples were cleaned of dust by

filtering through a 0.8 µm pore-size membrane filter. The intensity-intensity time-correlation functions were measured and then converted to the normalized electric field autocorrelation functions by means of the Siegert relation. The autocorrelation functions were analysed by the cumulant expansion and CONTIN methods. All the samples proved to be almost monodisperse with a polydispersity factor around 1.03.

Electrophoretic Mobility Measurements.

Malvern Zeta NanoZ equipment from Malvern Instruments was used to measure the electrophoretic mobility of the pNIPAM nanogels as a function of the temperature. The instrument uses a combination of laser Doppler velocimetry and phase analysis light scattering (PALS) in a technique called M3-PALS.[16] All measurements were done in 1 mM NaCl as background electrolyte. A total of ten runs were conducted for each measurement. Prior to each series, the instrument was always tested with Malvern zeta-potential transfer standard.

THEORETICAL BACKGROUND

Surface charge model of a non-draining colloid particle

According to the classical theory of electrophoretic mobility of colloid particles, the steady state motion of charged, spherical, non-draining particles in an electric field (*E*) can be described by taking into account that the electric force is balanced by the frictional force exerted on the surface of the particle by the liquid. If the thickness of the ionic atmosphere around the particle is negligible compared to the particle size the equality of the forces can be written as:

$$Q_{kin}E - 6\pi\eta a v_e = 0, \quad (1)$$

where Q_{kin} is sum of all charges present on the particle surface (electrokinetic charge), a is the radius of the particle, η is the viscosity of the medium and v_e is the particle velocity relative to the liquid (electrophoretic velocity). Eq. 1 is the simplest approximation to the electrophoretic velocity of a charged particle. When the ionic atmosphere around the particle is too thick it introduces a correction to Eq. 1 called the electrophoretic retardation force. The applied field acts not only on the charges present on the particle surface but also on the oppositely charged small ions present in the diffuse layer. Since these ions move to the opposite direction they cause a liquid flow which slows down the movement of the central charged particle. Taking into account the additional retardation force the electrophoretic velocity can be expressed as:

$$v_e = \frac{Q_{kin}E}{6\pi\eta a} + \frac{2E}{3\eta}\int_a^\infty \rho r dr \quad (2)$$

where ρ is the charge density in the double layer. For relatively thin double layer using the Smoluchowski solution the electrophoretic mobility ($u_e = v_e/E$) of the particle can be expressed as

$$u_e = \frac{Q_{kin}}{4\pi\eta\kappa a^2}\left(1 + \frac{1}{\kappa a}\right)^{-1} \quad (3a)$$

$$u_e = \frac{Q_{kin}}{4\pi\eta\kappa a^2} \quad \text{if } \kappa a >> 1 \quad (3b)$$

w here κ^{-1} is Debey length (the thickness of the double layer).[17]

Elecrophoretic mobility of draining polyelectrolytes

The electrophoretic mobility of liquid-swollen charged colloid particles has initiated several investigations. These particle may contain charges distributed within their liquid swollen internal structure, which can contribute to the electrophoretic mobility of the particles. Ohshima has proposed a general theoretical framework that successfully combined the electrophoretic theories of spherical

hard particles and polyelectrolytes.[4] He treated the electrophoretic mobility of spherical soft particles that have a rigid core of radius *a*, coated by a polyelectrolyte layer with thickness *d*. To describe the frictional force acting on a particle he adopted the model of Debey and Bueche[18] that is the polymer segments were considered as resistance centres of radius a_p which are uniformly distributed within the polyelectrolyte layer at a volume number density N_p. This permeable porous layer exerts an overall frictional force ($-\gamma \boldsymbol{u}$) on the liquid flow ($\boldsymbol{u}$), where γ is the frictional coefficient of the polyelectrolyte layer. The frictional coefficient is related to the generaly used drag coefficient (λ) via the expression:

$$\lambda = \left(\frac{\gamma}{\eta}\right)^{1/2}$$

where η is viscosity of the liquid. λ^{-1} is also called the electrophoretic softness of the particle, which is the characteristic distance required for the flow to reduce from its value at the particle surface to the value characteristic within a thick polyelectrolyte layer. The general mobility expression derived by Ohshima assumes that the charge distribution of the polyelectrolyte layer has a spherical symmetry and the electric potential is low enough, so the linearized Poisson-Boltzmann equation can be used. Practically this means that the theory neglects any polarization effect. Several limiting cases of the general mobility expressions have been presented from which the following cases are used in the literature to interpret the experimental mobility data of microgel particles.

-*Spherical polyelectrolyte*: in the case of vanishing particle core ($a \to 0$) the particle becomes a spherical polyelectrolyte (a porous, permeable, charged sphere of uniformly distributed resistance centres). The exact form of the mobility expression is determined by the charge distribution within the particle. If it is assumed that the polyelectrolyte particle is uniformly charged the following mobility expression can be derived:

$$u_e = \frac{\rho_{fix}}{\eta\lambda^2}\left[1 + \frac{1}{3}\left(\frac{\lambda}{\kappa}\right)^2\left(1 + e^{-2\kappa b} - \frac{1-e^{-2\kappa b}}{\kappa b}\right) + \frac{1}{3}\left(\frac{\lambda}{\kappa}\right)^2 \frac{1+1/\kappa b}{(\lambda/\kappa)^2-1}\left\{\left(\frac{\lambda}{\kappa}\right)\frac{1+e^{-2\kappa b}-(1-e^{-2\kappa b})/\kappa b}{(1+e^{-2\lambda b})/(1-e^{-2\lambda b})-1/\lambda b} - (1-e^{-2\kappa b})\right\}\right] \quad (4)$$

where *b* is the radius of the spherical polyelectrolyte and ρ_{fix} is its uniform charge density. However, if all charges are accumulated at the surface of the particle providing a uniform surface charge density (σ_{fix}) for the permeable particle the resulting mobility expression is:[8]

$$u_e = \frac{\sigma_{fix}}{\eta\lambda^2}\left[\frac{3}{b} + \frac{8\pi}{b}\left(1 - \frac{\lambda b}{3}\frac{sinh(\lambda b)}{cosh(\lambda b) - [sinh(\lambda b)]/\lambda b}\right) + \frac{8\pi b\lambda^2}{3(1+\kappa b)}\right] \quad (5)$$

-*Large diameter particles with thick polyelectrolyte shell*: In this case the mobility expression is based on the observation that the potential within the polyelectrolyte layer can be approximated by the Donnan potential if $\kappa a >> 1$, $\lambda a >> 1$ as well as $\kappa d >> 1$ and $\lambda d >> 1$ hold and the polyelectrolyte layer has a uniform charge density (ρ_{fix}).[4,19] The model yields the following mobility expression:

$$u_e = \frac{\varepsilon_r\varepsilon_0}{\eta}\frac{\psi_0/\kappa_m + \psi_{DON}/\lambda}{1/\kappa_m + 1/\lambda} + \frac{\rho_{fix}}{\eta\lambda^2} \quad (6)$$

where ε_r is the relative permittivity of the solution, ε_o is the permittivity of a vacuum, Ψ_{DON} is the Donnan potential in the polyelectrolyte layer, Ψ_o is the potential at the boundary between the polyelectrolyte layer and the solution and κ_m is the effective Debye–Hückel parameter of the polyelectrolyte layer that involves the contribution of the polyelectrolyte charges:

$$\Psi_{DON} = \frac{kT}{ze} ln\left[\frac{\rho_{fix}}{2zen^{\infty}} + \left\{\left(\frac{\rho_{fix}}{2zen^{\infty}}\right)^2 + 1\right\}^{1/2}\right]$$

$$\Psi_0 = \frac{kT}{ze}\left(ln\left[\frac{\rho_{fix}}{2zen^{\infty}} + \left\{\left(\frac{\rho_{fix}}{2zen^{\infty}}\right)^2 + 1\right\}^{1/2}\right] + \frac{2zen^{\infty}}{\rho_{fix}}\left[1 - \left\{\left(\frac{\rho_{fix}}{2zen^{\infty}}\right)^2 + 1\right\}^{1/2}\right]\right)$$

$$\kappa_m = \kappa\left[1 + \left(\frac{\rho_{fix}}{2zen^{\infty}}\right)^2\right]^{1/4}$$

In the above equations *k* is the Boltzmann constant, *T* is the absolute temperature, *e* is the elementary charge, *z* is the valance of a symmetrical electrolyte present in n^{∞} concentration in the bulk phase.

In our calculations the temperature dependence of the permittivity in was taken from Lide,[20] while the data by Bingham and Jackson[21] were used to calculate the temperature dependence of the viscosity.

RESULTS AND DISCUSSION

The electrophoretic mobility of microgel beads is constrained by two limiting cases. One of them is the non-draining hard sphere limit, while the other one is the free draining limit of the gel beads. In the free-draining limit the polymer segments present in a gel particle are regarded as independent resistance centers of radius a_s distributed uniformly within the gel bead at a segment density N_s. It is assumed that the hydrodynamic interaction of the polymer segments can be neglected, thus each segment contributes the same Stokes resistance to the frictional coefficient (γ) of the microgel bead:[4]

$$\gamma = 6\pi\eta a_s N_s \tag{7}$$

The free draining limit is expected to be valid while the density of the polymer segments is low within the draining particle (high porosity). However, if the segment concentration increases hydrodynamic interactions develop, the flow slows down within the particle and the segments in the particle core

experience smaller drag force than the ones close to the particle surface. In the non-draining limit there is no flow through the gel bead due to the strong hydrodynamic interactions. The water present inside the microgel particle moves together with the gel bead, thus the inner polymer segments does not experience the drag force. This means that in this case only the surface segments contribute to the friction coefficient. As it is implied by the above summary the level of draining through the microgel particles has a profound effect on the drag force and thus on the electrophoretic mobility. Though, Ohshima's model provides a formal description of this effect with some limitation, it does not provide any guidance on the level of hydrodynamic interactions. Thus, in literature investigations the drag coefficient (λ) is usually described in terms of the polymer chain density either by using Brinkman's model,[22] or empirical expressions.[8,23]

Before going further, we should mention here that very recently new scaling arguments have been presented in the literature to interpret the molecular weight independence of the thermophoretic mobility of high molecular weight polymers.[12,13] It is a well-established fact that when the molecular weight of a polymer becomes large enough its thermal diffusion coefficient becomes molecular weight independent. This is wide-spreadly interpreted as the proof of the free-draining character of the polymer coil during thermal diffusion. The presented model however demonstrated that with increasing segment number the hydrodynamic interactions within the polymer coil diverge and the polymer coil becomes non-draining in a thermophoretic experiment. It was also shown that this leads to the experimentally observed molecular weight independence of the thermophoretic mobility. Since in the case of an electrophoretic mobility experiment the draining characteristics of the microgels also play an outstanding role, here we adopt the presented arguments to gain a better insight into the effect of hydrodynamic interactions on the electrophoretic mobility of the microgel particles.

Now, let us consider a microgel particle immersed into a dilute electrolyte solution. Let us assume that the microgel particle is built up by N_s polymer segments and each of them has the same Q_s charge compensated by monovalent mobile ions. When the microgel particle is exposed to an electric field ($\boldsymbol{E}$) each segment is influenced by a driving force $\boldsymbol{f_{E,s}} = Q_s * \boldsymbol{E}$. Since the polymer segments are connected with each other the total driving force acting on the gel network is $\boldsymbol{f_G} = N_s * \boldsymbol{f_{E,s}}$. This electrophoretic driving force causes the relative motion of the microgel particle to the liquid phase. If hydrodynamic interactions were not present then the water molecules and the small ions present in the solution could flow freely within the microgel particle and the microgel could move with a velocity characteristic for the individual segments. However, the moving segments drag liquid with themselves that produces a hydrodynamic force ($\boldsymbol{f_h}$) on each segment and small ion around them. The total hydrodynamic force exerted by the polymer network on a small ion within the microgel particle can be expressed as follows:

$$\boldsymbol{f_{h,i}} = 6\pi\eta a_i \langle \sum_j \boldsymbol{u_j}(\boldsymbol{r_{ij}}) \rangle \tag{8}$$

where a_i is the small ion radius, $\boldsymbol{u_j}$ is the flow field around segment j, $\boldsymbol{r_{ij}}$ is the distance of segment j from the small ion i, and <·> is the average over polymer configurations.

Another force that acts on small ions is the electrophoretic driving force ($\boldsymbol{f_{E,i}} = e * \boldsymbol{E}$, assuming a monovalent ion, where e is the elementary charge). The fate of a small ion within the microgel is determined by the ratio of the two forces. If the hydrodynamic force is much smaller than the

electrophoretic force the small ion can move freely through the gel bead. However, if the hydrodynamic force dominates the small ion is dragged with the gel network. To judge, which scenario could be expected within the microgel particles, we have to express the ratio of these forces. As it has been shown if due to $\boldsymbol{f_{E,s}}$ all polymer segments move with the same electrophoretic velocity ($\boldsymbol{v_E}$) the hydrodynamic force exerted by them within the gel bead can be expressed as:[12]

$$\boldsymbol{f_{h,i}} = -\frac{N_S a_i}{R_h}\boldsymbol{f_{E,s}} \tag{9}$$

where R_h is the hydrodynamic radius of the gel bead. Since a microgel is a chemically crosslinked polymer network, it is built up by n_{ch} pieces of sub-chains connected by the cross-links. For the sake of simplicity we may assume that each polymer sub-chain contains $N_{s,ch}$ segments between two cross-links, thus the number of polymer segments within the microgel can be written as $N_s=n_{ch}*N_{s,ch}$, while the volume of the microgel can be expressed as $V\sim R_h^3\sim n_{ch}R_{s,ch}^3$, where $R_{s,ch}$ is the hydrodynamic radius of a sub-chain. It should be noted that though the size of the charged sub-chain ($R_{s,ch}$) depends on many factors such as its number of segments, its charge density, ionic strength and temperature, under given conditions it has a well-defined finite value. Using the latter expression to express the hydrodynamic radius of the microgel (R_h) eq.9 can be rewritten as

$$\boldsymbol{f_{h,i}} = -\frac{n_{ch}^{2/3} N_{s,ch} a_i}{R_{h,ch}}\boldsymbol{f_{E,s}}\sim n_{ch}^{2/3}\boldsymbol{f_{E,s}} \tag{10}$$

Dividing this expression with the electrophoretic driving force acting on a small ion we get

$$\frac{\boldsymbol{f_{h,i}}}{\boldsymbol{f_{E,i}}}\sim n_{ch}^{2/3}. \tag{11}$$

What eq. 11 reveals is that when n_{ch} >> 1 the hydrodynamic force dominates within the microgel particle, thus small ions and solvent molecules are dragged with the polymer network as it moves in an electric field. In other words the microgel core is non-draining, and the flow lines are pushed out of the particle inner core to its surface layer. At the same time if electrochemical potential gradients are present the small ions are free to diffuse in or out of the microgel. This also means that if $\kappa^{-1}<<R_h$ any volume element within the microgel core must be electro-neutral. Combining the non-draining character of the particle core and its electroneutrality, we can conclude that the charges present in the microgel core do not contribute to its electrophoretic mobility.

Between the non-draining core and the external fluid always there must be a transition layer. As it has been shown the thickness of this layer ($L\sim\lambda^{-1}$) is inversely proportional to the square root of the segment density within the polymer. This means that its actual magnitude is strongly affected by the swelling of the microgel particle, which in turn depends on the cross-link density of the gel ($N_{s,ch}$), and the swelling of the sub-chain ($R_{s,ch}$) that is affected by e.g. the temperature, pH and ionic strength. Altogether, as the particle swelling increases (the segment density decreases) the transition layer becomes thicker and as a consequence more charge will contribute to the electrophoretic mobility of the microgel.

To test the reliability of the above model predictions and to compare them with the predictions of the non-draining hard sphere model and the draining polyelectrolyte model, we prepared microgel

particles with four different internal charge distribution: 1. 'uncharged' microgel particles (N), 2. uniformly charged microgels (C), and core/shell microgels 3. with uncharged core and uniformly charged shell (N-C) and 4. with uniformly charged core and uncharged shell (C-N).

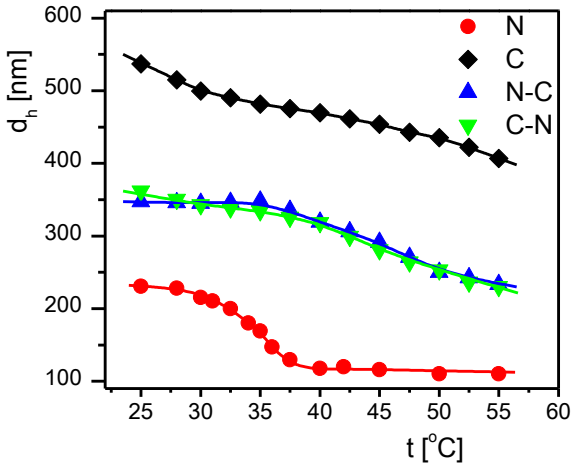

Figure 1. The hydrodynamic size of the microgel particles as a function of temperature at pH = 7.0 in 1 mM NaCl solution. The acronyms indicate the following microgel electric structure: N - uniform uncharged, C - uniform charged, N-C - neutral core with charged shell, C-N - charged core with neutral shell.

In Fig. 1 the effective hydrodynamic diameter of the particles is plotted against the temperature. In good agreement with the literature data[1] the uniform neutral pNIPAm particles (N) collapse in a narrow ~5 °C temperature range starting near 32 °C. The particles shrink from 230 nm to 110 nm and their size does not change further with increasing temperature. Also in agreement with the literature data[1] the diameter of the uniformly charged microgel particles (C) is significantly larger than that of the neutral particles due to the electrostatic interactions between the ionic carboxyl groups. At room temperature the hydrodynamic volume of the charged gel particles is approximately an order of magnitude larger than that of the neutral ones. Since the presence of the 10% charged monomers in the polymer network makes the particles more hydrophilic the collapse temperature of the charged particles increases and under the investigated conditions (pH = 7, I = 1mM) it actually shifts above the studied temperature range.

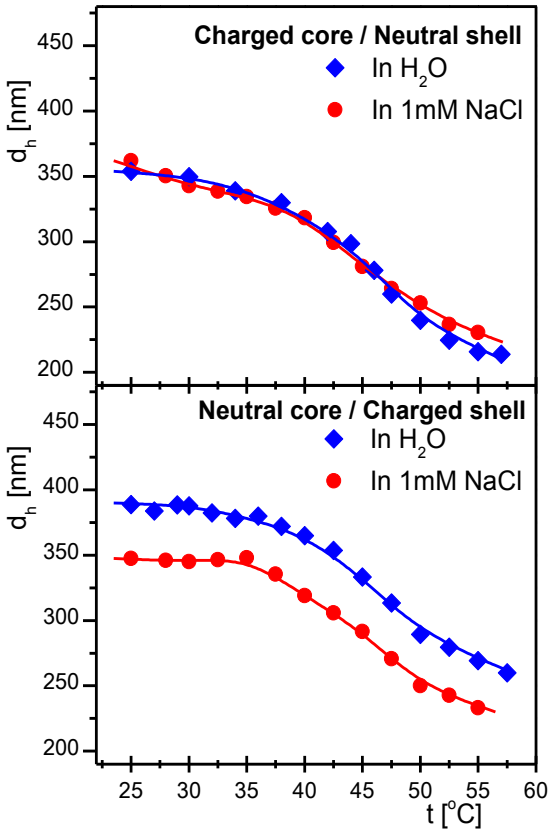

Figure 2. The hydrodynamic size of the core-shell microgel particles as a function of temperature at pH = 7.0 in Milli-Q water and in 1 mM NaCl solution.

As it may also be expected the hydrodynamic size of the core-shell particles falls in between that of the neutral and uniformly charged particles. However, it is more surprising that the hydrodynamic size of the core/shell particles seems unaffected by the localization of the charges within the gel beads and the swelling curves coincide for the charged core and the charged shell particles. Since this coincidence is rather counterintuitive we repeated the measurements at pH=7 without the addition of sodium chloride to enhance the electrostatic interaction. The results are plotted in Fig.2. and as it can be seen in the figure the decreased ionic strength does not affect the particle swelling significantly when the particle core is charged and the shell is uncharged (CN) but it has large effect when the core is neural but the shell of the gel particles is charged (NC). This clearly indicates that the charges are localized differently in the two core /shell particles. To interpret these observations we have to remember that the crosslinker monomer builds in faster into the growing polymer chains leading to the formation of a more crosslinked inner region and a less or non-crossliked outer regions on the pNIPAm microgel particles when they are prepared with a classical batch polymerization.[14,24] As a consequence when the ionic monomers are co-polymerized in the shell, at the end of the synthesis a barely crosslinked charged outer shell forms. The swelling of this outer shell is highly sensitive to the changes of the ionic strength since the charged dangling chains can extend further away from the microgel core due to the increased electrostatic interaction at lower ionic strength resulting in a larger hydrodynamic size. At the same time when the charged monomers are situated in the core of the microgel particles the charged chains are surrounded with a highly crosslinked uncharged shell and a loosely crosslinked

uncharged outer shell. When the ionic strengths is decreased the less crosslinked outer chains of the charged core may extend into the uncharged shell (if they are not chemically anchored to the inner part of the uncharged shell due to chain transfer reactions during the synthesis) but at the same time the outer loosely crosslinked uncharged pNIPAm chains that are responsible for the hydrodynamic size of the particles will be insensitive to the ionic strength. Thus we can conclude that though the hydrodynamic size of the two types of core-shell microgels arbitrarily coincide at pH=7 and 1mM ionic strength but the lowength swelling measurements confirm the expected core/shell structure of the prepared microgel particles.

In Fig.3 the electrophoretic mobility of the different microgel particles is plotted against the temperature. The 'neutral' pNIPAm particles also have an electrophoretic mobility because they have charges originating from the initiator.[3] At room temperature the mobility of the uniformly charged (C) and charged shell (N-C) microgel particles is the same with significantly higher negative value than that of the uniform uncharged microgel (N). The mobility of the charged core – uncharged shell (C-N) microgel is between the mobility values of the neural core – charged shell (N-C) and neutral particles. Since the core/shell particles have practically identical size (see Fig.1), furthermore they contain similar amount but differently localized charges, this observation implies that when the charges are localized in the core of the gel particle they contribute to the electrophoretic mobility in a smaller extent than the charges in the shell. The mobility increases with increasing temperature in all cases due to the decreasing size of the particles.

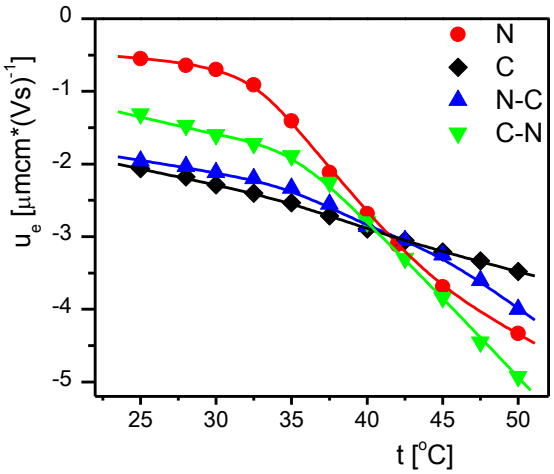

Figure 3. Electrophoretic mobility of the microgel particles as a function of temperature at pH = 7.0 in 1 mM NaCl solution. The acronyms indicate the following microgel electric structure: N - uniform uncharged, C - uniform charged, N-C - neutral core with charged shell, C-N - charged core with neutral shell.

As it has already been demonstrated in the literature, both the draining (eq.4-6) and the non-draining (eq.3) models can be fitted to the experimental mobility data. Unfortunately, we found that in the case of the draining models the fitting parameters (the electrokinetic charge and electrophoretic softness) are strongly correlated, thus instead of using an ambiguous fitting procedure we tried to analyse the

data with a different approach. Since at pH=7 the carboxylic groups present in the microgel particles are fully dissociated, the total charge of the gel particles remains constant regardless of the particle swelling. Since eq.3 allows the unambiguous calculation of the electrokinetic charge of the microgels from the available experimental data as a first step we determined the charge predicted by the non-draining hard sphere model in the function of the microgel swelling and evaluated if the results are consistent with the non-draining core / draining thin shell prediction we derived based on the scaling analysis of the hydrodynamic interactions. To highlight the relative changes of the predicted charge, the calculated values are normalized by the charge predicted at 50 C for each type of microgel. The results are plotted in Fig.4.

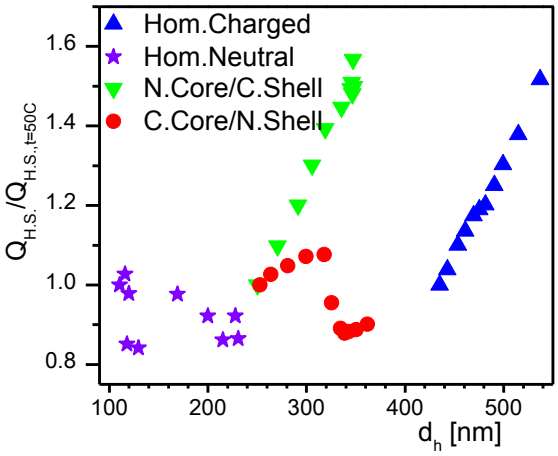

Figure 4. The electrokinetic charge of the microgel particles given by the non-darning hard sphere model and normalized by the value calculated at t=50C in the function of particle swelling. (N.Cor/C.Shell indicates the microgel prepared with uncharged core and charged shell, while C.Core/N.Shell indicates the microgel with charged core and uncharged shell).

In the case of the 'uncharged' microgel particles the calculated electrokinetic charge does not show any systematic changes with increasing microgel size. This is in good agreement with the expectation that in this case the charges originating from the initiator tend to accumulate at the interface of the microgel. The calculated electrokinetic charge corresponds to ~600 charged groups on the particle surface, which is ~50% of the number of charges found by titration on similar type microgel particles.[6,25] However, this observation is consistent with the non-draining character of the particle, because as we discussed before charges can be localized in the non-draining core of the microgel without contributing to the electrophoretic mobility.

In the case of the homogenously charged microgel and the core/shell microgel with homogenously charged shell, the hard-sphere non-draining model indicates similarly increasing surface charge with microgel swelling. This observation is in agreement with the argument that with particle swelling the thickness of the draining surface layer increases because such a thickening layer should result in an increasing amount of charged groups present in the draining surface layer, thus in increasing electrokinetic charge. At the same time the electrokinetic charge does not level off even for the most

swollen core/shell microgel, which indicates that the thickness of the draining layer is smaller than the thickness of the outer charged layer of the core/shell microgel.

Finally we should note that the microgel particle prepared with a charged core and uncharged shell show unique changes in their electrokinetic charge. Though these changes may seem rather peculiar at a first sight they are actually in good agreement with our considerations. With initial swelling the calculated electrokinetic charge slightly increases then at an intermediate size it suddenly drops to a smaller value than the initial charge at 50 C. Finally this is followed again by a very small increase of the electrokinetic charge. To interpret these results we have to remember that pNIPAm microgel particles are not uniformly crosslinked but there are less crosslinked dangling chains both on the outer surface if the charged core and on the uncharged shell. Furthermore, at high temperature the outer uncharged shell is in a collapsed state. This allows some of the outer dandling chains of the charged core to reach the microgel surface providing some surface charge. With decreasing temperature the charged particle core can swell further, which can deliver more charges of charged core to the microgel surface layer resulting in the slightly increasing electrokinetic charge. When the temperature becomes low enough, the outer uncharged shell also swells and it swells beyond the dangling charges of the core, which will get inside the non-draining internal part of the gel particle this way. Since the swollen outer shell does not contain copolymerized charges the amount of charges in the draining outer shell drops with the swelling of the uncharged shell as it is indicated by the results. With the swelling of the uncharged shell the draining surface layer gets thicker however this results only in a minor increase of the electrokinetic charge, presumably due to the penetration of the dangling chains of the charged core into the uncharged shell.

As a next step we also wanted to test if the draining models could provide a physically consistent interpretation of the experimental results. Since at pH=7 the total charge of the gel particles (Q_{gel}) remains constant regardless of the particle swelling, if these charges are localized at the surface of or distributed uniformly within a draining particle, then the surface charge density (σ_{fix}) or the volume charge density (ρ_{fix}) can be expressed in terms of the analytical charge (Q_{gel}) and the hydrodynamic radius (R_h) of the particle:

$$\sigma_{fix} = \frac{Q_{gel}}{4\pi R_h^2} \qquad \text{or} \qquad \rho_{fix} = \frac{3Q_{gel}}{4\pi R_h^3} \tag{12}$$

This means that if the charge of the gel particle is measured the electrophoretic softness of the gel beads can be determined using the experimental mobility and hydrodynamic size data. Unfortunately this approach cannot be used for the core/shell particles because in that case the volume of the swollen charged shell is unknown, thus the charge density in eq.6 cannot be estimated reliably. Thus in the remaining part of the paper we focus on the ‘uncharged’ and the homogenously charged microgels.

The draining models can formally provide the hydrodynamic description of the moving microgel particles ranging from the free draining case to the non-draining limit. The latter case is represented

by a diverging drag coefficient ($\lambda \to \infty$). It is straightforward to show that in this case eq.4 reduces to (assuming that $R_h = b$):

$$u_e = \frac{\rho_{fix}}{3\eta\kappa^2}\left(1 + e^{-2\kappa R_h} - \frac{1-e^{-2\kappa R_h}}{\kappa R_h}\right) \tag{13a}$$

$$u_e = \frac{\rho_{fix}}{3\eta\kappa^2} = \frac{Q_{gel}}{4\pi\eta(\kappa R_h)^2 R_h} \qquad \text{if } \kappa R_h >> 1 \tag{13b}$$

while eq.5 reduces to:

$$u_e = \frac{\sigma_{fix}}{\eta}\frac{8\pi R_h}{3(1+\kappa R_h)} \tag{14a}$$

$$u_e = \frac{8\pi}{3\eta\kappa}\sigma_{fix} = \frac{2Q_{gel}}{3\eta\kappa R_h^2} \qquad \text{if } \kappa R_h >> 1 \tag{14b}$$

Comparing eq.13b end eq.14b to eq.3b reveals that the mobility expressions provided by the non-draining limit of the draining models are not identical with the mobility expression derived for a charged hard sphere. Instead for a given mobility and hydrodynamic size the following relationships hold between the electrokinetic charge values provided by the different models:

$$Q_{Hom} \approx \kappa R_h Q_{H.Sp.} \qquad (\kappa R_h >> 1,\ \lambda R_h >> 1 \text{ and } \lambda >> \kappa) \tag{15}$$

$$Q_{Surf} \approx \frac{3}{8\pi} Q_{H.Sp.} \qquad (\kappa R_h >> 1,\ \lambda R_h >> 1 \text{ and } \lambda >> \kappa) \tag{16}$$

where $Q_{H.Sp.}$ is the electrokinetic charge given by the charged hard sphere model, Q_{Hom} and Q_{Surf} are the electrokinetic charge values given by the non-draining limit of the draining particle models for homogenous and surface charge distribution, respectively. It is also interesting to note that Pelton et al. have already found that the non-draining model required around 20 times less charge than the spherical polyelectrolyte model to reproduce the experimental mobility value in the case of their investigation.[3] Substituting the hydrodynamic size (200-300 nm) and the Debey-Hückel parameter (10^8 m^{-1}) they had into eq.15, the κR_h value is around 20-30, which is in good agreement with the ratio they found for $Q_{Hom}/Q_{H.Sp.}$.

Taking into account that the non-draining limit represents the maximum drag for a draining particle, the electrokinetic charge determined by eq.13 or eq.14 is the upper limit for the microgel charge a

specific model can provide at a given mobility value. As a first test we compared these upper limits to the estimated analytical charge of the microgels. To derive the analytical charge of the microgel particles we used potentiometric titrations to determine the charge of the 'neutral' and the homogenously charged microgel particles, which were found 3.8 μeq/g and 805 μeq/g, respectively. In previous investigations the microgel molar mass was found to be in the range of 2-5x10^8 g/mol.[26] Using these values as lower and upper limits we converted the titration results into the charge of the individual microgel particles. The results are plotted in Fig.5a where the estimated range of particle charge is plotted as a light blue and a light yellow band for the 'uncharged' and the homogenously charged microgels, respectively.

As it is discussed in the literature the charges of the 'uncharged' microgel is originating from the persulfate initiator and it tends to accumulate at the particle surface. In line with this generally accepted view, the non-draining limit of the draining surface charge model is also plotted in Fig.5a (blue spheres). However, as it is shown in the figure the kinetic charge predicted in this case is far below the expected analytical charge of the particle regardless of the microgel swelling. This means that the draining surface charge model (eq.5) cannot explain the experimental mobility data of the 'uncharged' microgel. However, it can be argued that only a portion of the charges are situated at the surface of the microgel and the rest is distributed within the particle. In this case following the arguments of Fernández-Nieves et al.,[8] the mobility of the microgel can be given as the sum of the surface contribution (eq.5) and the core contribution (eq.4). To test this possibility we also calculated the non-draining limit of the homogenously charged draining particle model (blue stars), which provided larger electrokinetic charge than the expected analytical charge. This means that by fitting the electrophoretic softness of the microgel in eq.4 the constant electrokinitic charge of the microgel can be maintained as the function of swelling. To test this approach we have chosen an electrokinetic charge value in the middle of the expected range (2x10^{-16} C/particle) as the object function and fitted the electrophoretic softness (λ^{-1}) using eq.4, eq.5 and eq.12 to recover this charge in the function of particle swelling. It should be noted that our calculation indicated that the surface charge contribution to the overall mobility was negligible compared to the charged core contribution in this representation. The results of the approach are plotted in Fig.5 by black stars; the electrokinetic charge used in the fitting is shown in Fig.5a, while the fitted electrophoretic softness values are shown in Fig.5b. As it could be expected the fitted electrophoretic softness values increase with microgel swelling and the fitted values are in good agreement with previous results.

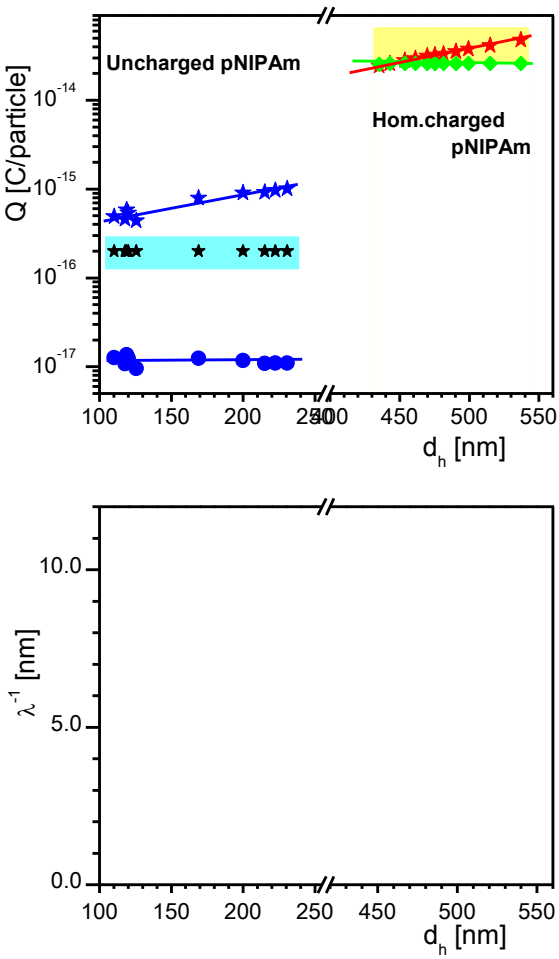

Figure 5. Top panel: The electrokinetic charge of the microgels given by the non-draining limit of the draining surface charge model (blue spheres for uncharged pNIPAm), and the non-draining limit of the homogenously charged draining particle model (blue stars for uncharged pNIPAm and red stars for homogenously charged pNIPAm). The electrokinetic charge used to fir the electrophoretic softness is plotted by black stars for the uncharged pNIPAm and by green diamonds for the charged ones. The range of microgel charge estimated from the titration is plotted as light blue and light yellow bands for the 'uncharged' and the homogenously charged microgels, respectively. Bottom panel: The electrophoretic softness fitted for the uncharged microgel (black stars) and for the homogenously charged microgels (green diamonds).

As a next step we extended this approach to the homogenously charged microgels. As it is shown in Fig.5a the upper limit for the microgel charge provided by the non-draining limit of the draining homogenously charged sphere model (eq.4; red stars) is in the range where the analytical charge of the microgel is estimated from the titration (light yellow band). Choosing the lower limit of the estimated analytical charge of the homogenously charged microgel (green diamonds) we fitted the electrophoretic softness of the microgels to keep the charge constant with particle swelling. The fitted electrophoretic softness data are plotted in Fig.5b (green diamonds). Though, with increasing swelling the softness again increases, the electrophoretic softness of the charged microgel is found much smaller than the values fitted for the 'uncharged' particles. Taking into account that the charged microgels are highly swollen in the investigated temperature range, while the 'uncharged microgel' is fully collapsed at high temperatures these results seem to contradict to the physical model that the

level of draining (the electrophoretic softness) is related to the segment density within the particle. It should also be noted that the highly swollen state of the charged microgel at the highest investigated temperature has another implication: with further temperature increase the microgel can further shrink and the maximum charge the model (eq.13) can predict should decrease. Since the lower limit of the predicted analytical charge has already coincided with the upper limit of the electrokinetic charge allowed by the model, it can be expected that at higher temperatures the model cannot predict as much charge as it is expected from the titration data as it is shown by the red and the green lines in Fig.5a.

CONCLUSIONS

To conclude, we presented scaling arguments to show that the hydrodynamic interactions in the core of a microgel particle exceeds the electrophoretic driving force in low ionic strength media. As a consequence the core of the gel particles becomes non-draining and it is expected that the counterions of the charged network present in this non-draining core are dragged with the microgel particle and the particle core behaves as a neutral hard core in an electrophoretic experiment. The electrophoretic charge of the microgels is provided by a thin draining shell, whose thickness increases with particle swelling. To challenge both the physical picture implied by the scaling arguments and the generally applied draining models we prepared pNIPAm-based microgel particles with different internal electric structures and measured their mobility and hydrodynamic size as a function of microgel swelling. Our data imply that though the draining models can be used to fit the electrophoretic mobility data, the fitted parameters does not seem physically coherent when the results gained for an 'uncharged' and for a homogenously charged microgel are compared. At the same time when in line with the predictions of the scaling arguments it is assumed that the microgels have a non-draining core and a thin draining shell whose thickness increases with particle swelling, the experimental data are in good agreement with the model predictions. To get a better understanding how the electrophoretic mobility of the charged microgels vary with particle collapse it would be desirable to perform the measurements in a wider temperature range. Unfortunately our experimental setup did not allow this.

AUTHOR INFORMATION

Corresponding Author

*E-mail: imo@chem.elte.hu.

ACKNOWLEDGMENTS

This work was supported by the Hungarian Scientific Research Fund (OTKA K100762 & K116629) and by NanoS3 Marie Curie Initial Training Network, funded through the European Union Seventh Framework Programme (FP7 ITN) under grant agreement no. 290251.

REFERENCES

(1) Pelton, R. H. Temperature-sensitive aqueous microgels. *Adv. Colloid Interface Sci*. **2000**, *85*, 1-33.

(2) Hoare, T.; Pelton. R. Functional Group Distributions in Carboxylic Acid Containing Poly(N-isopropylacrylamide) Microgels. *Langmuir*, **2004**, *20*, 2123–2133.

(3) Pelton, R. H.; Pelton, H. M.; Morphesis, A.; Rowell, R. L. Particle sizes and electrophoretic mobilities of poly(N-isopropylacrylamide) latex. *Langmuir* **1989**, 5, 816-818.

(4) Ohshima, H. Electrophoresis of soft particles. *Adv. Colloid Interface Sci.* **1995**, 62, 189-235.

(5) Ohshima, H.; Makino, K.; Kato, T.; Fujimoto, K.; Kondo, T.; Kawaguchi, H. Electrophoretic Mobility of Latex Particles Covered with Temperature-Sensitive Hydrogel Layers. *J. Colloid Interface Sci.* **1993**, 159, 512-514.

(6) Gilányi, T.; Varga, I.; Mészáros, R.; Filipcsei, G.; Zrínyi M. Preparation and characterization of monodisperse NIPA microgels. *Phys. Chem. Chem. Phys.* **2000**, *2*, 1973-1977.

(7) Nabzar, L.; Duracher, D.; Elaıssari, A.; Chauveteau, G.; Pichot, C. Electrokinetic Properties and Colloidal Stability of Cationic Amino-Containing N-Isopropylacrylamide-Styrene Copolymer Particles Bearing Different Shell Structures. *Langmuir* **1998**, *14*, 5062-5069.

(8) Fernández-Nieves, A.; Fernández-Barbero, A.; de las Nieves, F. J.; Vincent, B. Motion of microgel particles under an external electric field. *J. Phys.: Condens. Matter*, **2000**, *12*, 3605-3614.

(9) Fernández-Nieves, A.; Márquez, M. Electrophoresis of ionic microgel particles: From charged hard spheres to polyelectrolyte-like behavior. *J. Chem. Phys.* **2005**, *122*, 084702-084702-6.

(10) Gilányi, T.; Varga, I.; Mészáros, R.; Filipcsei, G.; Zrínyi, M. Interaction of Monodisperse Poly(N-isopropylacrylamide) Microgel Particles with Sodium Dodecyl Sulfate in Aqueous Solution. *Langmuir*, **2001**, *17*, 4764–4769.

(11) Hoare, T.; Pelton. R. Electrophoresis of functionalized microgels: morphological insights. *Polymer*, **2005**, *46*, 1139-1150.

(12) Morozov, K. I.; Köhler, W. Thermophoresis of Polymers: Nondraining vs Draining Coil *Langmuir*, **2014**, *30*, 6571–6576.

(13) Yang, M.; Ripoll, M. Driving forces and polymer hydrodynamics in the Soret effect. *J. Phys.: Condens. Matter* **2012**, *24*, 195101.

(14) Wu, X; Pelton, R. H.; Hamielec, A. E.; Woods D. R.; McPhee W. The kinetics of poly(*N*-isopropylacrylamide) microgel latex formation. *Colloid Polym. Sci.* **1994,** *272*, 467-477.

(15) Jones, C. D.; Lyon L. A. Synthesis and Characterization of Multiresponsive Core−Shell Microgels. *Macromolecules* **2000**, *33*, 8301-8306.

(16) Malvern Instrument Ltd., *ZetaSizer NanoZ User Manual*, Worcestershire, WR14 1XZ, United Kingdom, **2004**.

(17) Stigter D. in "*Enriching Topics from Colloid and Surface Science*" ed. van Olphen, H K.; Mysels J. Theorex, La Jolla, **1975**, pp. 293-307.

(18) Debye, P.; Bueche, A. Intrinsic Viscosity, Diffusion, and Sedimentation Rate of Polymers in Solution *J. Chem. Phys.* 1948, *16*, 573.

(19) Ohshima, H. Theory of Electrostatics and Electrokinetics of Soft Particles, *Sci. Technol. Adv. Mater.* **2009**, *10*, 063001.

(20) Lide, D. R. *Handbook of Chemistry and Physics*; 78th ed.; CRC Press: New York, **1997-1998**.

(21) Bingham, E. C.; Jackson R. F. *Bull. Bur. Stds.* **1918**, *14*, 75.

(22) Brinkman, H. C. Problems of fluid flow through swarms of particles and through macromolecules in solution, *Research* **1949**, *2*, 190-194.

(23) Carman, P.C. Fluid Flow though Granular Beds. *Trans. Inst. Chem. Eng.* **1937**, *15*, 150-166.

(24) Acciaro, R.; Gilanyi, T.; Varga, I. Preparation of Monodisperse Poly(N-isopropylacrylamide) Microgel Particles with Homogenous Crosslink Density Distribution. *Langmuir*, **2011**, *27*, 7917-7925.

(25) McPhee, W.; Tam, K.C.; Pelton, R. Poly(N-isopropylacrylamide) Latices Prepared with Sodium Dodecyl Sulfate. *J. Coll. Int. Sci.* **1993**, *156*, 24-30.

(26) Varga, I.; Gilányi, T.; Mészáros, R.; Filipcsei, G.; Zrínyi, M. Effect of Cross-Link Density on the Internal Structure of Poly(*N*-isopropylacrylamide) Microgels. *J. Phys. Chem. B* **2001**, 105, 9071-9076.